ARKIV FÖR FYSIK Band 15 nr 32

Communicated 11 March 1959 by Erik Rudberg and Kai Siegbahn

Electron binding energies in uranium

By Carl Nordling and Stig Hagström

With 3 figures in the text

ABSTRACT

The L_{III}, M_{II}–M_V and N_I–N_V level energies in uranium have been measured with the photo electron method. Only a minority of the corresponding X-ray absorption edges have been observed. The binding energies of these shells, which range from 17 keV down to 700 eV, have been determined in this study with an accuracy of a few tenths of an electron volt. Energy values of the K and L levels are deduced by adding energies of X-ray lines to the pertinent binding energies as measured in the present investigation, and an observed discrepancy for the L_{III} energy is discussed.

Introduction

The photo electron method of determining the energies of inner electron levels has recently been developed to such an accuracy as to make it compete favourably with the X-ray absorption method. Precision measurements of K and L level energies have been made for elements of the 4th, 5th and 6th periods (1, 2, 3). However, determinations have been made only exceptionally of the binding energies of more than one shell for each element. In the present investigation we have extended the application of the photo-electron method to an element in the last period of the periodic system, viz. uranium, and precision measurements are made of several levels in this element. Altogether, ten energies in the L, M and N shells have been measured. The earliest attempt to determine the binding energies of uranium with the photo electron method was made by Robinson in 1925 (4). The accuracy of these measurements was lower by a factor of about one hundred than that of the present investigation. X-ray absorption spectra in uranium have been studied as far out as in the M shell, where Lindberg measured the M_{III}, M_{IV} and M_V absorption limits with an accuracy of about $1:10^3$ (5).

A detailed description of the experimental arrangement and the principles of the photo electron method has previously been given in references (1, 2, 3, 6).

Experimental

The photo electron sources were prepared as thin evaporated layers on an aluminum backing, 15 μ thick. Throughout the measurements the $A6$ Auger line of copper served as a calibration line (1). The $B\varrho$ value of this line, 283.803 ± 0.010 gauss-cm, was

Table 1.

X-ray line	Wavelength (x.u.)	Energy (eV)
Cu $K\alpha_1$	1537.396	8047.5
Ge $K\alpha_1$	1251.48	9886.1
Pd $K\alpha_1$	584.240	21176.6
Ag $K\alpha_1$	558.253	22162.4

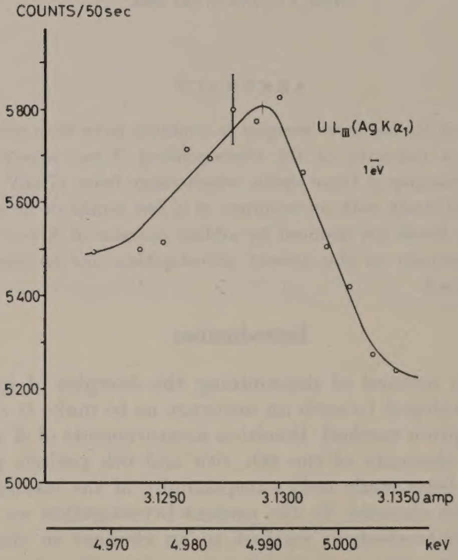

Fig. 1. $UL_{III}(AgK\alpha_1)$ photo line.

Table 2. $U L_{III}$ $(Ag K\alpha_1)$, $U L_{III}$ $(Pd K\alpha_1)$.

Anode	#	$I_{UL_{III}}$ (amps)	I_c (amps)	$B\varrho$ (gauss-cm)	E_{photo} (eV)	B.E. + ϕ_{sp} (eV)
Ag	131	3.12945	3.71933	238.795	4990.5	17171.9
Ag	134	3.12950	3.72006	238.752	4988.6	17173.8
Pd	135	2.80050	3.71786	213.781	4003.6	17173.0
Ag	135	3.12802	3.71802	238.771	4989.4	17173.0
Ag	136	3.12805	3.71771	238.792	4990.3	17172.1
					Mean:	17172.8 ± 0.7

$U L_{III}$: B.E. + $\phi_{sp} = 17172.8 \pm 0.8$ eV

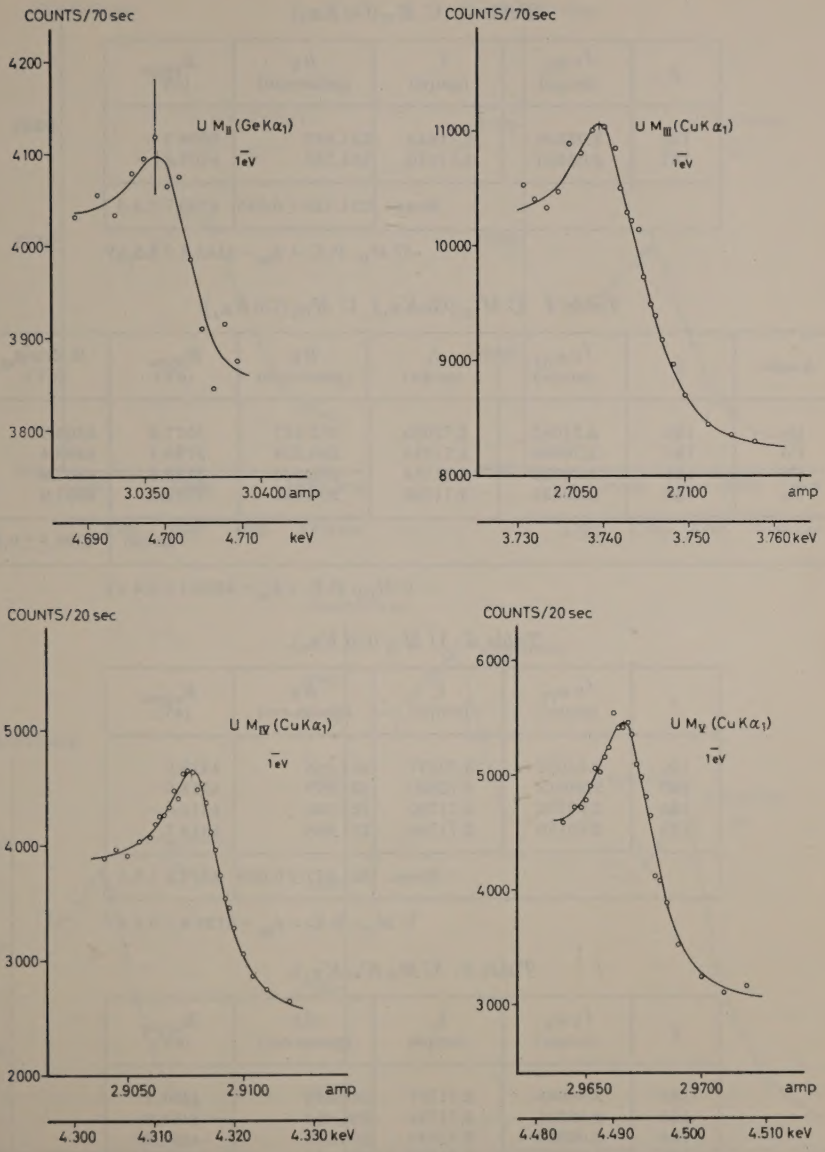

Fig. 2. Photo lines from *M* shells in uranium.

Table 3. U M_{II} (Ge $K\alpha_1$).

#	$I_{\mathrm{U}\,M_{\mathrm{II}}}$ (amps)	I_c (amps)	$B\varrho$ (gauss-cm)	E_{photo} (eV)
135	3.03550	3.71845	231.682	4698.9
137	3.03555	3.71716	231.767	4702.4
		Mean:	231.725 ± 0.085	4700.7 ± 3.5

U M_{II}: B.E. + $\phi_{\mathrm{sp}} = 5185.4 \pm 3.5$ eV

Table 4. U M_{III} (Ge$K\alpha_1$), U M_{III} (Cu$K\alpha_1$).

Anode	#	$I_{\mathrm{U}\,M_{\mathrm{III}}}$ (amps)	I_c (amps)	$B\varrho$ (gauss-cm)	E_{photo} (eV)	B.E. + ϕ_{sp} (eV)
Ge	130	3.31085	3.72093	252.527	5577.8	4308.3
Cu	135	2.70608	3.71788	206.574	3739.1	4308.4
Cu	135	2.70622	3.71784	206.586	3739.6	4307.9
Cu	136	2.70632	3.71796	206.587	3739.6	4307.9
					Mean:	4308.1 ± 0.3

U M_{III}: B.E. + $\phi_{\mathrm{sp}} = 4308.1 \pm 0.4$ eV

Table 5. U M_{IV} (Cu $K\alpha_1$).

#	$I_{\mathrm{U}\,M_{\mathrm{IV}}}$ (amps)	I_c (amps)	$B\varrho$ (gauss-cm)	E_{photo} (eV)
130	2.91022	3.72077	221.983	4315.3
130	2.91018	3.72090	221.972	4314.9
135	2.90772	3.71790	221.964	4314.6
135	2.90770	3.71784	221.966	4314.7
		Mean:	221.971 ± 0.008	4314.9 ± 0.3

U M_{IV}: B.E. + $\phi_{\mathrm{sp}} = 3732.6 \pm 0.4$ eV

Table 6. U M_{V} (Cu $K\alpha_1$).

#	$I_{\mathrm{U}\,M_{\mathrm{V}}}$ (amps)	I_c (amps)	$B\varrho$ (gauss-cm)	E_{photo} (eV)
135	2.96688	3.71791	226.478	4491.1
135	2.96698	3.71784	226.490	4491.6
135	2.96920	3.72080	226.479	4491.2
136	2.96658	3.71752	226.479	4491.2
		Mean:	226.482 ± 0.005	4491.3 ± 0.2

U M_{V}: B.E. + $\phi_{\mathrm{sp}} = 3556.2 \pm 0.4$ eV

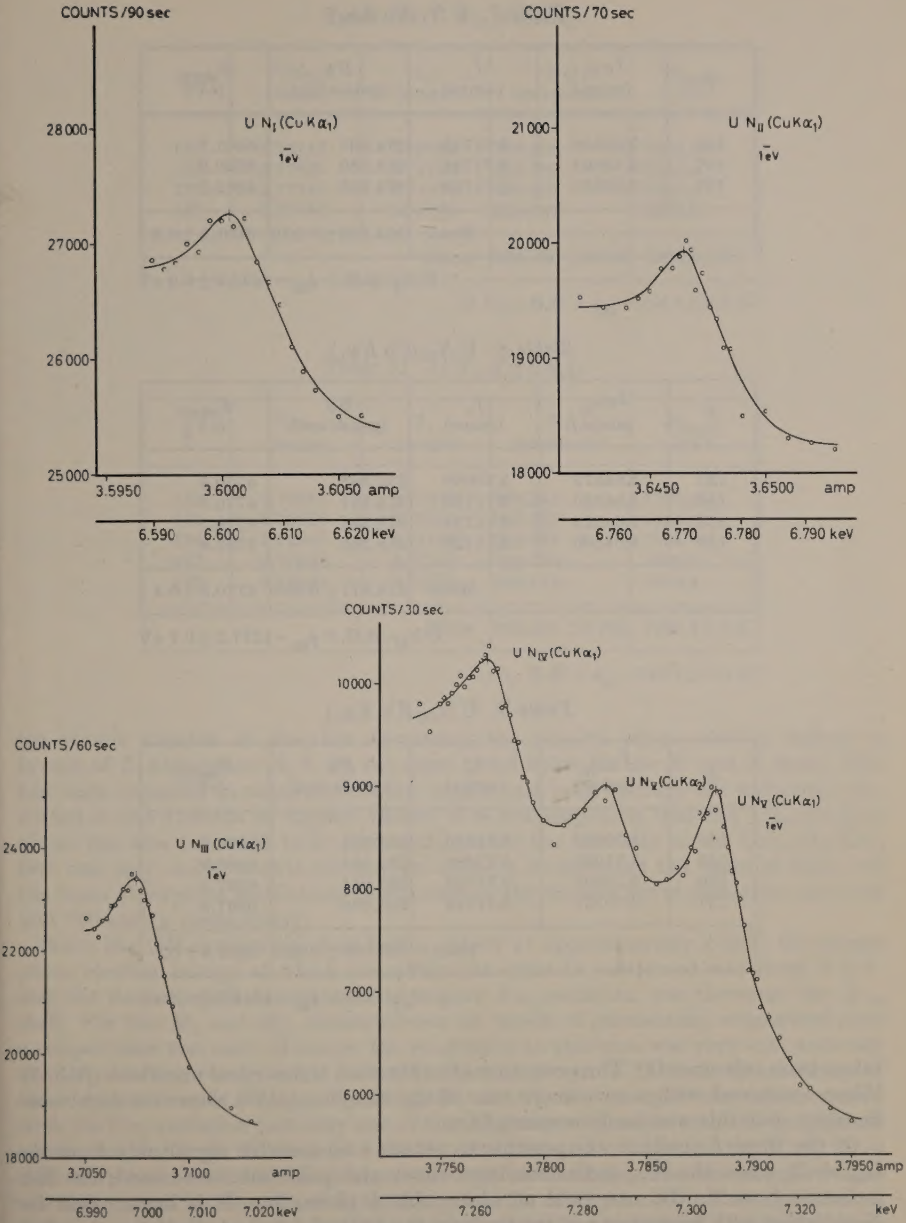

Fig. 3. N photo lines of uranium excited with Cu $K\alpha_1$-radiation.

Table 7. U N_{I} (Cu $K\alpha_1$).

#	$I_{\mathrm{U}N_{\mathrm{I}}}$ (amps)	I_c (amps)	$B\varrho$ (gauss-cm)	E_{photo} (eV)
136	3.60046	3.71752	274.867	6601.7
137	3.59992	3.71724	274.850	6600.9
137	3.60035	3.71726	274.878	6602.2
		Mean:	274.865 ± 0.016	6601.6 ± 0.8

U N_{I}: B.E. + $\phi_{\mathrm{sp}} = 1445.9 \pm 0.9$ eV

Table 8. U N_{II} (Cu $K\alpha_1$).

#	$I_{\mathrm{U}N_{\mathrm{II}}}$ (amps)	I_c (amps)	$B\varrho$ (gauss-cm)	E_{photo} (eV)
135	3.64972	3.72080	278.382	6770.5
136	3.64650	3.71752	278.381	6770.5
137	3.64623	3.71724	278.382	6770.5
137	3.64600	3.71726	278.363	6769.6
		Mean:	278.377 ± 0.009	6770.3 ± 0.4

U N_{II}: B.E. + $\phi_{\mathrm{sp}} = 1277.2 \pm 0.7$ eV

Table 9. U N_{III} (Cu $K\alpha_1$).

#	$I_{\mathrm{U}N_{\mathrm{III}}}$ (amps)	I_c (amps)	$B\varrho$ (gauss-cm)	E_{photo} (eV)
135	3.70860	3.71840	283.055	6998.2
135	3.71095	3.72080	283.052	6998.0
136	3.70802	3.71796	283.044	6997.6
137	3.70737	3.71724	283.050	6997.9
		Mean:	283.050 ± 0.005	6997.9 ± 0.2

U N_{III}: B.E. + $\phi_{\mathrm{sp}} = 1049.6 \pm 0.5$ eV

taken from reference (2). The procedure of calibration is described elsewhere (6, 3, 7). When examined with a microscope, one of the samples (#136) showed a slight nonlinearity, but this was easily corrected for.

Of the three L shells it was possible to obtain a measurable signal only from the L_{III} shell, when the $K\alpha_1$ radiations from silver and palladium were used, the $K\alpha$-radiation from tin did not yield an observable L photo line. It is known that for X-radiation with frequency not too far from the critical L frequency of the absorber, the L_{III} photo absorption is the dominating one, and as the X-ray frequency inreases

Table 10. $\mathrm{U}\,N_{\mathrm{IV}}\,(\mathrm{Cu}\,K\alpha_1)$.

#	$I_{\mathrm{U}N_{\mathrm{IV}}}$ (amps)	I_c (amps)	$B\varrho$ (gauss-cm)	E_{photo} (eV)
135	3.78115	3.72080	288.406	7263.4
136	3.77800	3.71796	288.386	7262.4
137	3.77747	3.71724	288.401	7263.2
137	3.77757	3.71726	288.407	7263.5
		Mean:	288.400 ± 0.010	7263.1 ± 0.5

$\mathrm{U}\,N_{\mathrm{IV}}$: B.E. $+ \phi_{\mathrm{sp}} = 784.4 \pm 0.7$ eV

Table 11. $\mathrm{U}\,N_{\mathrm{V}}\,(\mathrm{Cu}\,K\alpha_1)$.

#	$I_{\mathrm{U}N_{\mathrm{V}}}$ (amps)	I_c (amps)	$B\varrho$ (gauss-cm)	E_{photo} (eV)
135	3.78968	3.71840	289.244	7305.4
135	3.79210	3.72080	289.242	7305.2
136	3.78910	3.71796	289.233	7304.8
137	3.78846	3.71724	289.240	7305.2
137	3.78855	3.71726	289.246	7305.4
		Mean:	289.241 ± 0.005	7305.2 ± 0.2

$\mathrm{U}\,N_{\mathrm{V}}$: B.E. $+ \phi_{\mathrm{sp}} = 742.3 \pm 0.6$ eV

(or atomic number of absorber decreases), the relative photo yield is shifted in favour of L_{I} absorption (4, 8, 9); the same trend holds for the M and N shells. This has been reported in reference (1) for copper and molybdenum $K\alpha$ radiation converted in the L shells of copper. Hence, it is not surprising that the $\mathrm{U}L_{\mathrm{II}}(\mathrm{Sn}\,K\alpha_1)$ photo line was too weak to be observed because the intensity of the $\mathrm{U}L_{\mathrm{III}}(\mathrm{Ag}\,K\alpha_1)$ line was only ≈ 700 counts per minute above a background ten times as high, and the mass absorption coefficients in uranium of the tin and silver radiations are ≈ 65 and 100 cm^2/g respectively.

Since the GM-counter window had a cut-off at approximately 2 keV, the lowest photo electron energy at which measurements could be performed was about 3 keV, and the deepest shell accessible with copper $K\alpha_1$ radiation was therefore the M_{III} shell. For the M_{I} and M_{II} measurements an anode of germanium, evaporated onto a copper base was used. However the conversion in this case was very low, and only the M_{II} binding energy could be determined; as shown in Table 3, the accuracy of these measurements is poor. The M_{III}–M_{V} and N_{I}–N_{V} energies were all measured with $\mathrm{Cu}\,K\alpha_1$ radiation (actually one of the M_{III} runs was made with the germanium anode, see Table 4). Table 1 lists the wavelengths and energies of the X-ray lines that have been used for the production of photo electrons. The wavelength values are those given by Sandström in the Encyclopedia of Physics (10). The experimental data for each shell are listed in Tables 2–11. In cases in which the $K\alpha_1$ radiation from more than one X-ray target was used, the anodes are listed in the first column. The

Table 12.

Shell	B.E. (eV)	Shell	B.E. (eV)
U L_{III}	17168.3	U N_{I}	1441.4
U M_{II}	5180.9	U N_{II}	1272.7
U M_{III}	4303.6	U N_{III}	1045.1
U M_{IV}	3728.1	U N_{IV}	779.9
U M_{V}	3551.7	U N_{V}	737.8

next column lists the number of the sample, followed by the currents of the photo line and calibration line (CuA6 Auger line), $B\varrho$ value of photo line (corrected for residual magnetic field (2)), energy of photo line and (Tables 2 and 4) binding energy including work function of spectrometer material (2). The binding energies, *B.E.*, of the various shells, corrected for work function of spectrometer, 4.5 eV, are listed in Table 12. Figures 1–3 show photo lines from the ten uranium shells investigated.

Error estimation

Because of the different counting statistics and signal-to-background ratios obtained from the various shells, it could not be assumed that all measurements were performed with the same relative accuracy. Hence, the errors assigned to the mean values of momentum and energy in the tables are derived from the reproducibility of the corresponding sequence of measurements. We have preferred to take the errors twice as large as the standard deviations:

$$\Delta x = \pm 2 \sqrt{\frac{\sum (x-\bar{x})^2}{n(n-1)}}. \qquad (1)$$

This corresponds to a risk level of about 15 per cent in cases in which four measurements have been made; for the M_{II} binding energy, which was measured only twice, the risk level is about 30 per cent. Below each table is given the binding energy of the shell including work function of spectrometer material. Here the error given for the binding energy includes not only that derived from the reproducibility, but also the error given in reference (2) for the CuA6 Auger line.

"Absolute" energy determination

Recently, measurements of the L X-ray spectrum of uranium have been performed by Merrill and DuMond with relative errors of about 10 ppm (11). From their data it is possible to obtain the energy difference between the M_{V} and N_{III} levels with an accuracy of one part in 10^4. These two levels were chosen for an "absolute" energy determination with the method orginally proposed by K. Siegbahn (12). The U M_{V} (Cu $K\alpha_1$) and U N_{III} (Cu $K\alpha_1$) lines were recorded in the same measurement. Employing the energy difference of the $L\gamma_3$ and $L\beta_9$ lines 2507.1 ± 0.3 eV, taken from the X-ray data in reference (11), the $B\varrho$ values and energies of these photo lines could be determined without the use of an additional reference line. The relevant data are listed in Table 13 together with the results of the "relative" measurements, taken from Tables 6 and 9. Here, as well as in the other measurements of this investigation,

Table 13. U M_V U N_{III} (Cu $K\alpha_1$).

Photo line	I (amps)	$B\varrho$ (gauss-cm)	E_{photo} (eV)	E_{photo} (eV) Tables 6 and 9
U M_V (Cu $K\alpha_1$)	2.96920	226.492 ± 0.032	4491.7 ± 1.3	4491.3 ± 0.4
U N_{III} (Cu $K\alpha_1$)	3.71095	283.067 ± 0.025	6998.8 ± 1.2	6997.9 ± 0.5

we have corrected for the effective residual magnetic field which is left along the electron trajectory when all external stray fields are balanced out at the center of the spectrometer. The method of applying this correction for an absolute energy calibration has been described in reference (2).

The accuracy of the U M_V U N_{III} (Cu $K\alpha_1$) calibration is rather low. It was shown in reference (2) that for unrelativistic energies a relative error in the current ratio α of the high energy line to the low energy line gives a relative error in momentum of the low energy line equal to

$$\frac{\Delta B\varrho_1}{B\varrho_1} = \pm \frac{\alpha^2}{\alpha^2 - 1} \cdot \frac{\Delta\alpha}{\alpha}. \tag{2}$$

The corresponding error for the high energy line is then:

$$\frac{\Delta B\varrho_2}{B\varrho_2} = \pm \frac{1}{\alpha^2 - 1} \cdot \frac{\Delta\alpha}{\alpha}. \tag{3}$$

It should be noticed that the *high* energy line has the smallest error. In fact, the error decreases asymtotically to zero for high current ratios α. The accuracy will then be limited by the uncertainties in the elementary constants and X-ray data.

The errors given in Table 13 for the two photo lines of the U M_V U N_{III} (Cu $K\alpha_1$) calibration are derived from equations (2) and (3) with a relative error of the current ratio equal to 5×10^{-5}. This is in agreement with the errors given in Tables 6 and 9 for the "relative" measurements of the M_V and N_{III} binding energies, and corresponds to an uncertainty in the localization of a photo line peak of approximately one thirtieth of the half width (defined as twice the width at half maximum intensity of the high energy flank). It is evident that the energies obtained from the "absolute" calibration are consistent with those determined relative the CuA6 Auger line.

Comparison with X-ray data

The comparison with X-ray data offered by the absolute energy determination described in the preceding section indicated a good agreement between the present measurements and those of X-ray spectroscopy. A more extensive comparison can be made if the three L binding energies are calculated by adding to the M and N binding energies, determined by the photo electron method (Table 12), the X-ray transition energies of the L spectrum, obtained from reference (11). In this way it was possible to get five determinations of the L_I energy, three of the L_{II} and four of the L_{III} energy. This is shown in Tables 14–16. The wavelength values given by Merrill and DuMond have been modified to become consistent with the wavelength

Table 14. L_{I} binding energy.

X-ray line	Transition	Energy of transition (11) (eV)	Energy of final state (Table 12) (eV)	Energy of initial state (eV)
$L\beta_4$	L_{I}–M_{II}	16574.1	5180.9	21755.0 ± 3.5
$L\beta_3$	L_{I}–M_{III}	17453.9	4303.6	21757.5 ± 0.5
$L\beta_9$	L_{I}–M_{V}	18204.1	3551.7	21755.8 ± 0.5
$L\gamma_2$	L_{I}–N_{II}	20483.3	1272.7	21756.0 ± 0.8
$L\gamma_3$	L_{I}–N_{III}	20711.2	1045.1	21756.3 ± 0.6
			Mean:	21756.1 ± 0.8

Table 15. L_{II} binding energy.

X-ray line	Transition	Energy of transition (11) (eV)	Energy of final state (Table 12) (eV)	Energy of initial state (eV)
$L\beta_1$	L_{II}–M_{IV}	17218.8	3728.1	20946.9 ± 0.5
$L\gamma_5$	L_{II}–N_{I}	19505.3[1]	1441.4	20946.7 ± 1.0
$L\gamma_1$	L_{II}–N_{IV}	20166.0	779.9	20945.9 ± 0.8
			Mean:	20946.5 ± 0.6

[1] The wavelength value 637.283 x.u. reported in reference (11) is apparently a misprint, the Bragg angle giving a value of 634.283 x.u.

Table 16. L_{III} binding energy.

X-ray line	Transition	Energy of transition (11) (eV)	Energy of final state (Table 12) (eV)	Energy of initial state (eV)
$L\alpha_2$	L_{III}–M_{IV}	13438.2	3728.1	17166.3 ± 0.4
$L\alpha_1$	L_{III}–M_{V}	13613.7	3551.7	17165.4 ± 0.4
$L\beta_6$	L_{III}–N_{I}	15725.1	1441.4	17166.5 ± 0.8
$L\beta_2$	L_{III}–N_{V}	16427.1	737.8	17164.9 ± 0.6
			Mean:	17165.7 ± 0.8

value 707.8310 x.u. of the Mo $K\alpha_1$ radiation, and the conversion factor from x.u. to eV is that given by DuMond and Cohen 1953 (13). The error given for each separate energy value is obtained by quadratic addition of the error given in reference (11) for the wavelength of the X-ray line and the error assigned to the quantity $B.E. + \phi_{\text{sp}}$ given below the pertinent table in this paper. The errors assigned to the mean values are twice as large as the standard deviations. It is seen that only two energy values deviate from the corresponding mean value by more than the error of the mean.

A comparison between the L_{III} energy, 17165.7 ± 0.8 eV, given in Table 16 and that of Table 12, 17168.3 ± 0.8 eV reveals a discrepancy which cannot be accounted for by the error limits. However, it should be kept in mind that the X-ray transition energies listed in Table 16 pertain to metallic uranium, whereas the samples studied in the present investigation were oxidized. This was shown by taking X-ray powder patterns from evaporated films. In order to get a sufficient amount of material, the uranium was evaporated onto an area of 5×5 cm^2 on a glass plate. Then the deposit was scratched off and put into the source holder of a Guinier camera. The patterns obtained from such samples showed that on evaporation the uranium had formed deposits of the oxide UO_2 which has a cubic structure with $a_0 = 5.4682$ Å (14). Moreover, it has been shown by Manescu that the L absorption edges of uranium are shifted in the oxides UO_2 and UO_3 (15). For the oxide UO_2 she found shifts in the L_I, L_{II}, and L_{III} absorption discontinuities of 7, 3.1 and 2.8 eV respectively. Hence, it cannot be precluded that the discrepancy observed for the L_{III} energy can be ascribed to "chemical" effects. This would indicate that the wavelengths of inner transitions in uranium should be affected by the chemical state of the element, since all energies measured with the photo electron method are referred to the Fermi level of the solid. Another possible explanation is that the final state of an X-ray transition is not necessarily identical with the corresponding ionization state created in the photoelectric process (20). I does not seem probable that the discrepancy can be attributed to uncertainties in the relative values of the resistors in the compensator (2). The conductivity of the irradiated uranium oxide is believed to be sufficiently high to prevent the samples from being electrically charged. This assumption is supported by the high reproducibility of the measurements on different samples. The uranium oxide UO_2 is a p-type semiconductor with an activation energy of 0.2 eV (21). Various conductivity values have been reported, ranging from $3.3 \cdot 10^{-1}$ to $6.3 \cdot 10^{-6}\ \Omega^{-1}\ \mathrm{cm}^{-1}$ (22).

The L absorption edges of uranium have been measured by Cauchois and Manescu (16), who report wavelength values for the L_I, L_{II} and L_{III} absorption discontinuities that correspond to energies of 21771.3 eV, 20944.6 eV and 17165.5 eV respectively ($E \cdot \lambda_s = 12372.2$ keV x.u.). The L_{III} energy is seen to be in good agreement with that of Table 16, whereas the L_I energy differs by as much as 15 eV from that of Table 14. However, the energies listed in Tables 14–16 are assumed to be related to the same level, viz. the Fermi level of the solid, whereas the final states of the various X-ray absorption edges are not identical. It seems probable that selection rules often play an important role for the transitions to the outer bands of a solid which are involved in the X-ray absorption process. These phenomena are discussed in detail in several references (17).

It is of great importance for nuclear spectroscopists to have reliable data on the binding energies of inner shells. Therefore, the K binding energy of uranium has been calculated in a similar way as the L energies in Tables 14–16. Ingelstam has determined the wavelengths of four X-ray lines in the K spectrum of urnaium (oxide) with an accuracy of 0.010 x.u. (18), and recently Beckman *et al.* measured the $K\alpha_1$ line in metallic uranium with limits of error as small as 0.004 x.u. (19). In Table 17 are listed the energies of these transitions, calculated from the wavelengths given in references (18) and (19). The corresponding K binding energies (Table 17) are obtained by adding the final state energies of the transitions as given in Tables 16 (L_{III}), 15 (L_{II}) and 12 (M_{III}, M_{II}). The L_{III} energy employed in the calculations is that of Table 16, since this value is the mean of four independent measurements.

Table 17. K binding energy.

X-ray line	Transition	Energy of transition (eV)	Energy of final state (see text) (eV)	Energy of initial state (eV)
$K\alpha_2$	K–L_{II}	94662.5[1]	20946.5	115609.0 ± 7.3
$K\alpha_1$	K–L_{III}	98437.4[1]	17165.7	115603.2 ± 7.8
$K\alpha_1$	K–L_{III}	98435.0[2]	17165.7	115600.8 ± 3.1
$K\beta_3$	K–M_{II}	110405.0[1]	5180.9	115585.9 ± 10.0
$K\beta_1$	K–M_{III}	111299.8[1]	4303.6	115603.4 ± 10.0
Weighted mean:				115601 ± 5

[1] Ingelstam (18) (oxide).
[2] Beckman *et al.* (19) (metal).

Because of the small error limits given in reference (19) for the $K\alpha_1$ line, we have preferred to give a weighted mean value of the K energy. The error assigned to the K energy has been calculated from the reproducibility of the results in the last column in Table 17. Here again, reservations must be made for the fact that the energies involved in the calculations are obtained from measurements on metallic uranium as well as uranium oxide. It should also be noticed that the *total* binding energy, i.e. the energy required for a complete removal of an electron from the solid includes the work function of the crystal. This quantity is usually of the order of 4 eV.

ACKNOWLEDGEMENTS

We are greatly indebted to Professor Kai Siegbahn for his kind interest and constant support. Further our thanks are due Fil. kand. Pär Bergvall for valuable discussions.

Institute of Physics, University of Uppsala.

REFERENCES

1. Sokolowski, E., Nordling, C. and Siegbahn, K., Arkiv f. Fysik *12*, 301 (1957).
2. Nordling, C., Arkiv f. Fysik *15*, 31 (1959).
3. Sokolowski, E., Arkiv f. Fysik *15*, 1 (1959).
4. Robinson, H. R., Phil. Mag. *50*, 241 (1925).
5. Lindberg, E., Nova Acta Reg. Soc. Sci. Upsal. *7* No. 7 (1931).
6. Nordling, C., Sokolowski, E. and Siegbahn, K., Arkiv f. Fysik *13*, 483 (1958).
7. Nordling, C., Arkiv f. Fysik *15*, 241 (1959).
8. Robinson, H. R., Proc. Roy. Soc. *104 A*, 455 (1923).
9. Hall, H., Rev. Mod. Phys. *8*, 358 (1936).
10. Sandström, A. E., in Encyclopedia of Physics XXX, 78, editor S. Flügge, Springer Verlag, Berlin (1955).
11. Merrill, J. J. and Du Mond, J. W. M., Phys. Rev. *110*, 79 (1958).
12. Siegbahn, K., Ark. Mat. Astr. Fys. *30 A*, 1 (1944).
13. Du Mond, J. W. M. and Cohen, R. E., Rev. Mod. Phys. *25*, 691 (1953).
14. X-ray powder data file, published by the American Society for Testing Materials.
15. Manescu, I., C.R. *225*, 537 (1947).

16. Cauchois, Y. and Manescu, I., C.R., *210*, 172 (1940).
17. Cauchois, Y., Journ. de Phys. *13*, 113 (1952).
—— Journ. de Chimie Phys. *51*, D 76 (1954).
Friedel, J., Proc. Phys. Soc. *66A*, 333 (1953).
Mott, N. F., Proc. Phys. Soc. *62A*, 416 (1949).
18. Ingelstam, E., Nova Acta Reg. Soc. Sci. Upsal. *10*, No. 5 (1936).
19. Beckman, O., Bergvall, P. and Axelsson, B., Arkiv f. Fysik *14*, 419 (1958).
20. Parratt, L. G., AFOSR TN-56-562, ASTIA AD 110,382 (ASTIA, Arlington Hall Station, Arlington 12, Virginia, U.S.A.).
21. Hartmann, W., Zeitschr. f. Physik 102, 709 (1936).
22. Meyer, W., Zeitschr. f. Elektroch. 50, 274 (1944).

Tryckt den 24 april 1959

Uppsala 1959. Almqvist & Wiksells Boktryckeri AB